Chin. J. Mech. Eng. (2017) 30:1447–1459
https://doi.org/10.1007/s10033-017-0198-x

REVIEW

Review of Large Spacecraft Deployable Membrane Antenna Structures

Zhi-Quan Liu[1] · Hui Qiu[1] · Xiao Li[1] · Shu-Li Yang[1]

Received: 28 February 2017 / Revised: 25 April 2017 / Accepted: 12 October 2017 / Published online: 7 November 2017

Abstract The demand for large antennas in future space missions has increasingly stimulated the development of deployable membrane antenna structures owing to their light weight and small stowage volume. However, there is little literature providing a comprehensive review and comparison of different membrane antenna structures. Space-borne membrane antenna structures are mainly classified as either parabolic or planar membrane antenna structures. For parabolic membrane antenna structures, there are five deploying and forming methods, including inflation, inflation-rigidization, elastic ribs driven, Shape Memory Polymer (SMP)-inflation, and electrostatic forming. The development and detailed comparison of these five methods are presented. Then, properties of membrane materials (including polyester film and polyimide film) for parabolic membrane antennas are compared. Additionally, for planar membrane antenna structures, frame shapes have changed from circular to rectangular, and different tensioning systems have emerged successively, including single Miura–Natori, double, and multi-layer tensioning systems. Recent advances in structural configurations, tensioning system design, and dynamic analysis for planar membrane antenna structures are investigated. Finally, future trends for large space membrane antenna structures are pointed out and technical problems are proposed, including design and analysis of membrane structures, materials and processes, membrane packing, surface accuracy stability, and test and verification technology. Through a review of large deployable membrane antenna structures, guidance for space membrane-antenna research and applications is provided.

Keywords Membrane antenna · Parabolic · Plane · Tensioning system · Dynamics

1 Introduction

With an increasing demand for large-aperture (hundreds of square meters or more) space-borne antennas, deployable membrane antennas have been attracting interest in space research areas. In comparison with traditional rigid antennas, membrane antennas can easily achieve larger scale with lighter weight, smaller stowage volume, and lower cost. At present, there are two main kinds of space-borne membrane antenna structures: parabolic and planar membrane antenna structures. These membrane antenna structures generally involve a membrane surface, support structures, and a tensioning system. Since 1970, a series of explorations of membrane antennas have been carried out in the United States, Europe, Japan, etc. Some progress has also been made in this domain over the past 10 years in China. However, up until now, no membrane antennas have been applied in space, except an American inflatable antenna with a diameter of 14 m that had space flight experience in 1996. It is obvious that applications of large membrane antennas in space still face many difficulties and challenges. In order to promote membrane antenna progress, it is necessary to review the development of deployable membrane antenna structures and provide guidance for space membrane-antenna researchers. Creative design and analysis of some

Supported by Research Fund of Institute of Spacecraft System Engineering, China Academy of Space Technology, China (Grant No. ZTBYY-7).

✉ Zhi-Quan Liu
liuzhiquanymj@sina.com

[1] Beijing Institute of Spacecraft System Engineering, China Academy of Space Technology, Beijing 100094, China

deployable structures and mechanisms were presented in Refs. [1–11], but deployable membrane antenna structures were not considered. Although structural characteristics and application prospects of inflatable antennas were summarized in Refs. [12–14], and advances in parabolic membrane antennas over the past decades were presented in Refs. [15, 16], characteristic comparisons were not considered among these membrane antenna structures. Additionally, Refs. [12–16] focused only on some special membrane antenna structures. So far, there has been little literature reviewing recent developments and providing a comprehensive comparison of different membrane antenna structures. Aimed at the problems described above, this paper presents recent advances, characteristic comparisons, technical problems, and future trends for large membrane antenna structures.

2 Advances in Deploying and Forming Methods for Parabolic Membrane Antennas

Parabolic membrane antennas are folded or wrapped when in stowed condition. When the spacecraft reaches its orbit, the antenna is deployed to the desired reflector surface according to flight procedures. At present, there are five methods for deploying and forming large parabolic membrane antennas, which are inflation, inflation-rigidization, elastic ribs driven, Shape Memory Polymer (SMP)-inflation, and electrostatic forming.

2.1 Inflation

A typical inflatable antenna structure is shown in Figure 1. The antenna is deployed by an inflation system mounted near the feed.

Since 1971, inflatable antennas with diameters of 7 m, 9 m, and 14 m have been developed by L'Garde, Inc. The 14 m-diameter inflatable antenna was selected for the flight experiment in May 1996 [17, 18], and its deployment procedure is shown in Figure 2. First, after the canister was opened (①→② in Figure 2), the three inflatable struts, membrane reflector, and clear canopy were pushed away from the canister by springs (② → ③ in Figure 2). Second, the struts and torus were inflated by gas provided by the inflation system in the canister (③ → ④ in Figure 2). Finally, after the struts and torus were fully inflated, the membrane reflector and clear canopy were inflated into a parabolic shape under inflation pressure and cable tension force (④ → ⑤ in Figure 2). When the antenna was fully deployed, the length of three struts was 28 m, and the whole antenna mass was 60 kg. The surface accuracy (root mean square (RMS) of axial deviation between the actual and design value of each point on the parabolic reflector) was measured to be 1.5 mm RMS in the central area with radius of 4 m [19].

Design parameters for inflatable antennas generally include inflation pressure, membrane thickness, elastic modulus of membrane material, boundary conditions, temperature, etc. In 2001, Greschik et al. [20] from the University of Colorado, investigated the influence of membrane thickness, membrane materials, thermal effects, boundary perturbations, and membrane wrinkles on surface accuracy, but the geometric differences of the membrane reflector shape during its deformation process were not considered in the calculation. In 2004, Naboulsi [21] from the Air Force Institute of Technology, carried out a detailed study on the main structure of an inflatable antenna (including the membrane reflector, inflatable struts, and torus) with the software ABAQUS. The results show that at higher inflation pressure, the surface shape error is greater, and asymmetric inflation pressure on the inflatable torus causes larger reflector surface deformations than symmetrical pressure. However, the effect of membrane wrinkles caused by the asymmetric inflation pressure on surface accuracy was not analyzed in this paper. In 2006, Xu et al. [22] from Zhejiang University, further analyzed the influence of inflation pressure and antenna focal length on reflector surface accuracy and proposed that surface

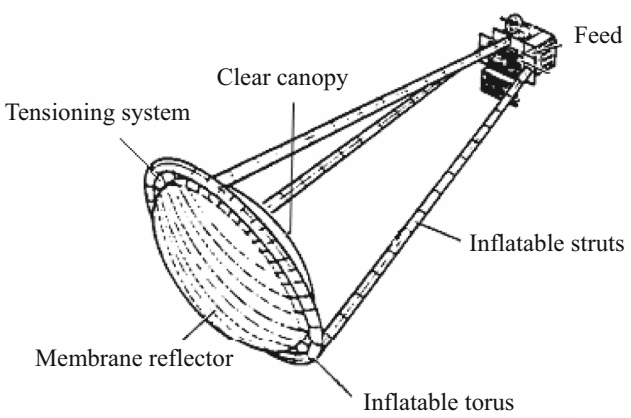

Figure 1 Inflatable antenna structure

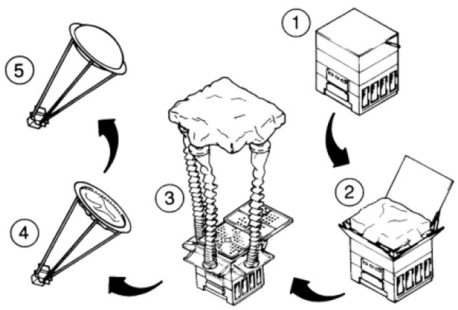

Figure 2 Deployment of inflatable antenna

accuracy could be adjusted by cable tension force. However, further studies that consider the cable deformations during the adjustment are still necessary. In 2012, Coleman et al. [23] from George Washington University, investigated the influence of edge forces and reflector diameters on reflector surface accuracy. For antennas with a diameter greater than 10 m, the influence of internal pressure on the surface accuracy is greater than the influence of edge forces. However, the membrane nonlinear property was not taken into account in the analysis. In 2015, Liu et al. [24] from Nanjing University of Aeronautics and Astronautics, used the Hamilton principle to deduce the frequency equation and mode function of inflatable antennas based on the Donnell nonlinear thin shell theory. However, changes in inflation pressure were ignored in the modal analysis.

In summary, the present design and analysis of inflatable antennas only focus on research on the influence of the relevant parameters for reflector surface accuracy. In-depth multi-objective structure optimization analysis and dynamic analysis of rigid-flexible coupling systems for spacecraft with large membrane antennas are required.

Inflatable antennas show great advantages owing to their light weights and small stowage volumes. However, the slow gas leakage in orbit requires a gas supplement system, leading to weight gain and short service life. Another disadvantage is that it is difficult for inflatable antennas to maintain the required surface accuracy under the alternating temperature conditions in space.

2.2 Inflation-Rigidization

In the process of inflation-rigidization, the membrane reflector is rigidized after being inflated to the desired parabolic shape and inflation pressure is released.

Since 1980, the European Space Agency (ESA) and the Contraves Space Division in Switzerland have carried out a series of studies on inflatable-rigidizable antennas. Contraves has developed antennas with diameters of 3.5 m, 6 m, and 12 m [25], as shown in Figure 3. The membrane reflector consisted of Kevlar fibers impregnated with a special polymer resin, and the area density was about 0.41 kg/m^2. Ground test results showed that the reflector surface was rigidized by solar radiation in six hours at the temperature of 110 °C, and the antenna achieved 0.98 mm RMS surface accuracy after being rigidized [26].

Inflatable-rigidizable antennas avoid some disadvantages faced by inflatable antennas, including decrease in surface accuracy, antenna performance degradation, and the requirement for a continuous gas supplement. However, their ability to maintain surface accuracy depends on further improvement of rigidizable material thermal stability, which is not good enough at present.

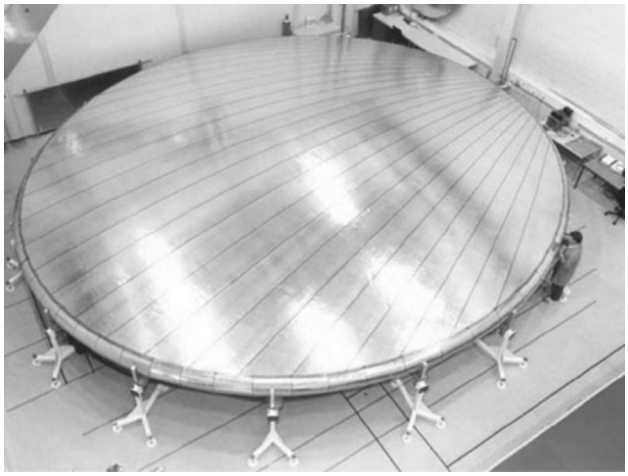

Figure 3 Contraves inflation-rigidization antenna

2.3 Elastic Ribs Driven

A fully deployed elastic ribs driven membrane antenna structure [27, 28] is shown in Figure 4. There are two steps to deploy the antenna. First, elastic ribs spiraled on the central hub release their elastic potential energy and then stretch out to become straight lines, which are in the same plane with the hub axis. Second, hinges installed in the connection between the elastic ribs and the central hub drive the elastic ribs to deploy radially like an umbrella, thus making the membrane reflector into a paraboloid.

In 2002, Pellegrino [29] from the University of Cambridge, developed an elastic ribs driven membrane antenna with a diameter of 1.5 m, which achieved a surface accuracy of 2.0 mm RMS, as shown in Figure 4. The reflector was composed of 12 elastic ribs, a central hub, and aluminized polyester film. When the antenna was folded, the ribs and film were twisted on the central hub and bound by rope. Once the rope was cut, the ribs released elastic potential energy to drive the membrane reflector deployment. Pellegrino designed the antenna diameter, focal length, surface accuracy, and membrane stress distribution and performed the deployment experiment. However, several elastic ribs were damaged because of an improper folding approach, and, in consequence, the 12 elastic ribs

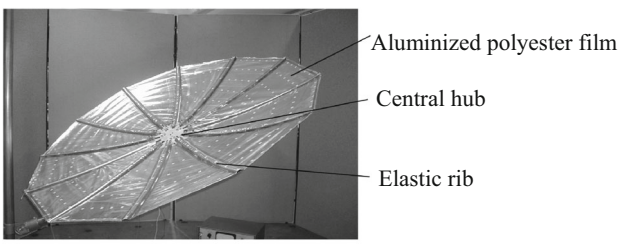

Figure 4 Elastic ribs driven membrane antenna

were deployed simultaneously. Therefore, further study is needed in antenna folding approaches.

Although elastic ribs driven membrane antennas are lightweight, the stiffness and surface accuracy is relatively low. In addition, deployment reliability is affected by complex movements, including the cutting of the rope before the ribs deploy and the rotation of ribs after their elastic potential energy is released.

2.4 SMP-Inflation

SMP-inflatable membrane antennas [30] are deployed and formed by the shape memory effect of SMP materials [31] and inflation. On the ground, the antenna is packed by an external mechanical load above the glass transition temperature of SMP material. Then, by keeping the external load constant and the temperature below the glass transition temperature, the antenna remains in the same state after unloading. When the spacecraft reaches its orbit, the membrane antenna is heated above the glass transition temperature, and the inflatable struts are inflated according to flight procedures. The reflector surface and torus are deployed gradually by shape recovery and thrust provided by the inflatable struts. Finally, the reflective surface returns automatically to the initial parabolic shape and is rigidized after the temperature drops below the glass transition temperature.

In 2007, Gaspar et al. [32] from NASA Langley Research Center, developed one SMP-inflatable membrane antenna, as shown in Figure 5. The antenna consisted of a 0.5 m diameter rigid parabolic reflector and a concentric annular membrane parabolic reflector with an outer diameter of 2 m. The area density of the SMP membrane was about 1.4 kg/m^2 and the thickness was 0.181 mm. The reflector surface accuracy was measured to be 1 mm RMS. James L. Gaspar et al. tested and simulated dynamic behaviors of the antenna structure. The results show that the first two modes are mainly determined by the tension force of the cables between the membrane reflector and torus and are irrelevant to the inflation pressure. However, the antenna apertures and membrane thickness were considered to be constant in this analysis.

SMP-inflatable membrane antenna deployment is driven by shape memory effect and inflation, of which the former dominates, and the antennas are rigidized after deployment. Thus, they have high reliability and strong surface accuracy maintaining ability. However, the heating power required during deployment is great (an antenna with a diameter of 35 m requires power of 67.77 kW), which is difficult to realize in the case of energy shortages.

2.5 Electrostatic Forming

The Astromesh antenna has successfully flown in space [33]. In order to further improve its surface accuracy, a gap is made between the membrane and the electrodes mounted on the front net of the Astromesh antenna structure, resulting in the formation of an electric field. Because of the electric field force, the metal-coated membrane is suspended on the front net and finally becomes a parabolic surface. The gap between the electrodes and membrane can be adjusted by the electrostatic force so as to actively control the reflector shape accuracy.

In 2004, SRS technologies and Northrop Grumman developed a 5 m diameter electrostatic forming membrane antenna [34], as shown in Figure 6. The antenna was composed of an Astromesh support structure, a membrane reflecting surface, electrodes, and a control system. The area density of the antenna structure was about 1 kg/m^2, and the surface accuracy was measured to be 1.1 mm RMS. In 2015, Zhang et al. [35] from Xidian University, optimized electrode configurations while taking membrane surface accuracy and system complexity as optimal targets, but the number of electrodes was assumed to be constant in the optimization. In the same year, Liu et al. [36], from Xidian University, established a theoretical model of membrane reflectors considering the coupled structural-electrostatic problem. The membrane surface accuracy and stress distribution uniformity were optimized based on the model, but the support structure elastic deformations were not taken into account in this paper.

The electrostatic-forming membrane antenna reflector surface can be controlled in real time by adjusting electrostatic forces, thus improving surface stability. Based on the mature Astromesh antenna technologies, electrostatic forming membrane antennas can theoretically be applied to large-sized and high-precision antennas in the future.

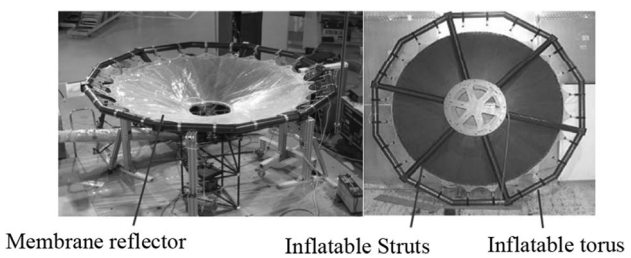

Figure 5 SMP-inflatable membrane antenna

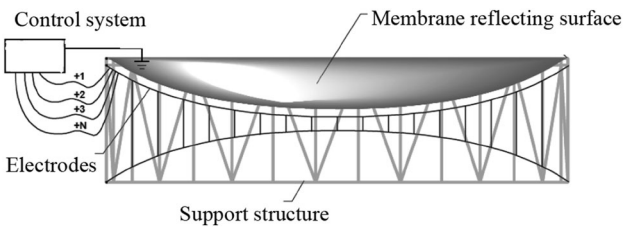

Figure 6 Schematic of electrostatic forming membrane antenna

Table 1 Comparison of parabolic membrane antennas with different deploying and forming methods

Type	Inflation	Inflation-rigidization	Elastic ribs driven	SMP-inflation	Electrostatic forming
Research departments	L'Garde in the USA	ESA and Contraves in Switzerland	University of Cambridge	NASA Langley Research Center	SRS and Northrop Grumman Xidian University
Application	In orbit	Prototype	Prototype	Prototype	Prototype
Aperture	14 m	12 m	1.5 m	2 m	5 m
Surface Accuracy	1.5 mm RMS	0.98 mm RMS	2 mm RMS	1 mm RMS	1.1 mm RMS
Area density	0.39 kg/m^2	0.41 kg/m^2	——	1.4 kg/m^2	~1 kg/m^2
Precision maintaining ability	Very low	Medium	Low	High	Very high
Packing factor	Very high	High	High	Medium	Medium
System complexity	Low	Medium	Medium	High	High
Pros	Light weight; Large packing factor	No need for gas after rigidization; Strong precision maintaining ability	Light weight	Strong precision maintaining ability; High deployment reliability	High surface accuracy; Strong precision maintaining ability
Cons	Gas leakage; Easily affected by alternating temperature conditions; Difficult to maintain surface accuracy; Short service life	Membrane wrinkles in rigidization process; Requires further improvement for material thermal stability	Low stiffness; Deployment reliability is affected by complex movements	Requires great heating power, which is difficult to realize in the case of energy shortages	Electrostatic damage and security risks of high voltage; Risks of winding

However, the antennas require high voltage (up to several thousand volts), which will bring electrostatic damage and safety risks to electronic products on the spacecraft. In addition, electrodes mounted on the front net might increase the risk of winding among the wires, membrane, and deployment mechanism of the support structure. Therefore, applications of this antenna technology in spacecraft are subject to many constraints at present.

Table 1 shows a comparison among parabolic membrane antennas with different deploying and forming methods. In general, advantages and disadvantages of each one are obvious, and some technical difficulties and risks need to be considered for space applications.

3 Membrane Materials for Parabolic Membrane Antennas

Parabolic membrane-antenna reflector materials are usually metal-coated polymer films. There are several requirements for the polymer film, including high elasticity modulus, high shear strength, low density, small thickness, high thermal stability, low thermal expansion coefficient, and strong space radiation resistance. Membrane materials commonly used in membrane antennas are polyester (PET) film and polyimide (PI) film [37–39]. Table 2 shows some typical performance parameters for these two kinds of polymer films.

As shown in Table 2, compared with polyester film, polyimide film has a larger modulus, higher tensile

Table 2 Properties of several kinds of membrane materials

Property	Units	PET Film			PI Film		
		Mylar 48	Mylar 75	Mylar 92	Kapton 20EN	Kapton 50EN	UPilex-25S
Thickness	μm	12	19	32	5	12.5	25
Destiny	g/cm^3	1.40	1.38	1.39	1.42	1.42	1.47
Modulus	GPa	3.79	3.79	3.79	5.0	5.0	9.1
Tensile strength	MPa	186 (MD)* 234 (TD)*	200 (MD) 244 (TD)	187 (MD) 276 (TD)	335	380	520
Thermal expansion coefficient	ppm/°C	20-60(50-200°C)			16 (50-200°C)	16 (50-200°C)	12 (50-200°C)
Elongation at break	%	110 (MD) 80 (TD)	130 (MD) 100 (TD)	140 (MD) 80 (TD)	55	62	42
Anti-ultraviolet radiation ability		Low			High		

* MD—Machine Direction; TD—Transverse Direction

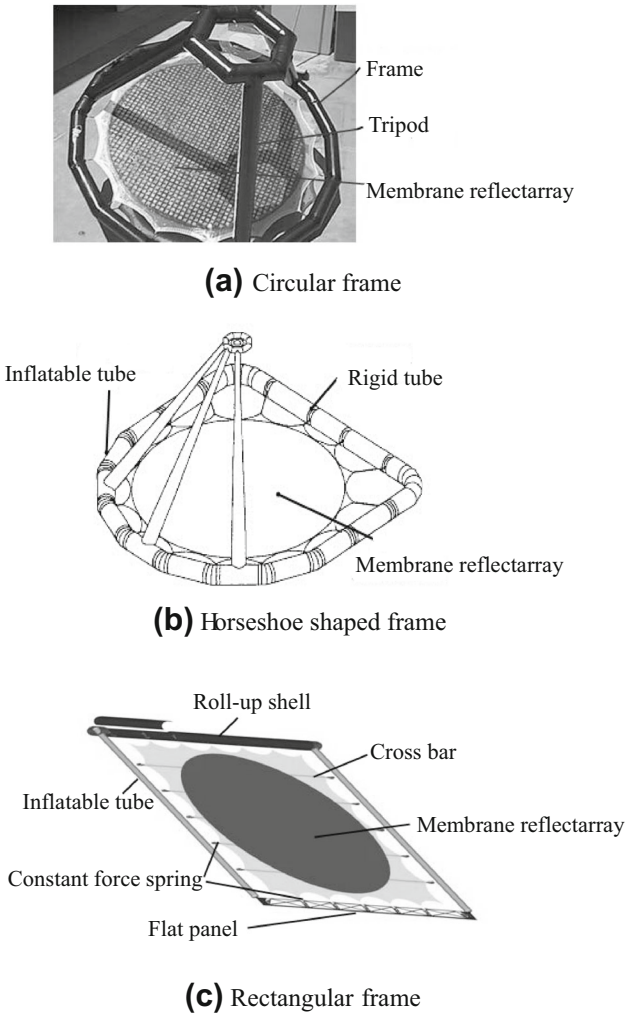

Figure 7 Structural configurations of planar membrane antennas

strength, lower thermal expansion coefficient, smaller elongation at break, and stronger anti-ultraviolet radiation ability. Therefore, polyimide film is considered to be a better candidate material in future space applications.

4 Development of Large Planar Membrane Antenna Structural Configurations

A typical planar membrane antenna structure is mainly composed of a deployable frame and a multi-layer flexible membrane, which is supported by the frame [40]. The multiple membrane layers are deployed to a planar structure with the deployment of the frame and maintain the required surface flatness through the tensioning system between the membrane and frame. Figure 7 shows the structural configurations of planar membrane array antennas developed in the USA between 1998 and 2008.

In 1998, Jet Propulsion Laboratory (JPL) and ILC Dover, Inc. developed a 1 m diameter X-band planar membrane reflect array antenna [41], as shown in Figure 7(a). The two-layer membrane was polyimide film with both sides clad with 0.5 μm thick copper. The frame was a circular inflatable tube, which was connected to a tripod supporting the antenna feed. In 2000, the two companies co-developed a 3 m Ka-band membrane reflect array antenna [42], as shown in Figure 7(b). The horseshoe shaped frame consisted of one straight rigid tube, two straight tubes, and one semi-circular inflatable tube. The membrane could be rolled on the rigid tube to avoid creases. There were 16 catenary points distributed on the horseshoe shaped frame to apply stress on the membrane, and the surface flatness was measured to be ± 0.2 mm. In

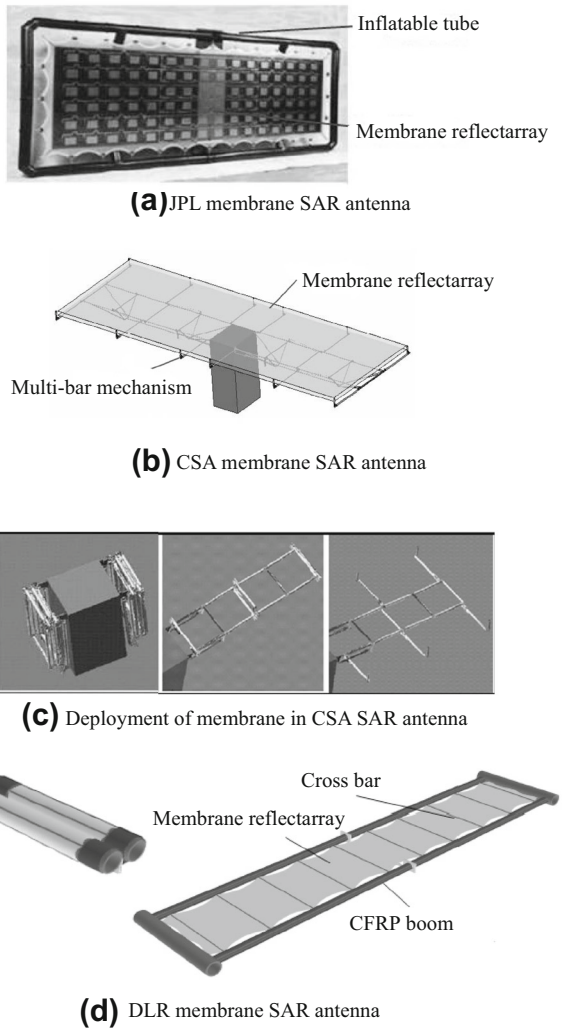

Figure 8 Membrane SAR antenna structures

2002, JPL proposed the idea of a "movie screen" membrane array antenna with a rectangular frame [44, 45], as shown in Figure 7(c). The antenna feed was offset on the spacecraft, which eliminated the need for a feed-supporting tripod, resulting in a more compact structure. Two edges of the rectangular frame were inflatable tubes, and the other two edges were flat panels covered by roll-up shells, on which the membrane could be tightly rolled. Several cross bars, distributed uniformly on the membrane and employed as compression members to stretch the membrane, had no connection with the inflatable tubes. One constant force spring hung on each end of the cross bar and was connected to cables at the membrane edge. Similarly, some constant force springs hung on the flat panel and were connected to the cable. The membrane was deployed by the tubes inflating and was tensioned by constant force springs after deployment. From 2004 to 2008, JPL conducted a series of studies on "movie screen" antennas [46–48]. In 2008, a 2.2 m × 2.2 m planar membrane antenna was developed and achieved a surface flatness of 0.17 mm.

In 2008, Guan et al. [49], from Zhejiang University, developed a 2 m × 2 m planar membrane antenna, whose structural configuration was similar to the one in Figure 7(c). The surface flatness was measured to be 0.32 mm. In 2012, Li et al. [50], developed a 6 m × 2 m L/C dual-band, single-layer planar membrane antenna, but the deployment was not considered for this paper.

In 1998, JPL put forward the membrane synthetic aperture radar (SAR) antenna concept [51–53]. In 2001, JPL, together with L'Garde and ILC Dover, developed two 3.3 m×1.0 m planar membrane passive phased array antennas [54], which consisted of three-layer membranes and were deployed by inflatable-rigidizable booms [55, 56], as shown in Figure 8(a). The area density of the one developed by L'Garde was 3.3 kg/m^2, and the antenna achieved ± 0.28 mm surface flatness. In 2011, JPL developed a 2.3 m × 2.6 m active phased array antenna [57], which reduced the number of membrane layers from three to two.

In 2007, the Canadian Space Agency (CSA) developed a 2 m × 3 m planar membrane SAR antenna with a three-layer membrane [58, 59], as shown in Figure 8(b). A multi-bar mechanism was adopted to realize two-dimensional antenna deployment [60], as shown in Figure 8(c). In 2008, the German Aerospace Center (DLR) developed a 6 m × 1.3 m membrane SAR antenna with a four-layer membrane, which was deployed by rollable carbon fiber reinforced polymer (CFRP) booms [61, 62]. The antenna structure configuration was similar to that in Figure 7(c), but cables at the membrane edges were connected directly to the CFRP booms instead of the cross bars. In 2012, in order to avoid boom deformations caused by cable tensile force, Straubel et al. [63] added cross bars to the antenna structure and both ends of the bars were interfaced with CFRP booms, as shown in Figure 8(d). These two parts had no connections in Figure 7(c).

The characteristics of the above-mentioned planar membrane antenna structural configurations are listed in Table 3. As shown by Table 3, planar membrane antenna frame shapes have changed from circular to horseshoe shape to rectangular. For planar membrane reflect array antennas with circular and horseshoe shaped frames, feeds need to be supported by tripods, which will block part of the electromagnetic wave reflection. Membrane antenna structures with rectangular frames are more compact because of the elimination of tripods. Therefore, there is an increasing tendency to use rectangular frames. In addition, CFRP and inflatable-rigidizable booms have good prospects for membrane antenna deployment.

Table 3 Comparison of planar membrane antenna structural configurations

Type	Year	Country	Band	Frame shape	Size (m)	Area density (kg/m^2)	Membrane layer No.	Deployment method	Surface flatness (mm)
Membrane reflect array antennas	1998	USA	X	Circle	1 (Aperture)	1.2	2	Inflatable booms	±1.3
	2000	USA	Ka	Horseshoe	3 (Aperture)	1.82	1	Inflatable booms	±0.2
	2008	USA	X/Ka	Rectangle	2.2×2.2	~3.5	3	Inflatable-rigidizable booms	≤0.17
	2012	China	L/C	Rectangle	6×2	–	1	–	–
Membrane phased array antennas	2001	USA	L	Rectangle	3.3×1.0	3.3	3	Inflatable-rigidizable booms	±0.28
	2007	Canada	C	Rectangle	2×3	–	3	Multi-bar linkage	–
	2011	USA	L	Rectangle	2.3×2.6	–	2	–	–
	2012	Germany	P	Rectangle	12.85×3.35	1.32	4	CFRP booms	–

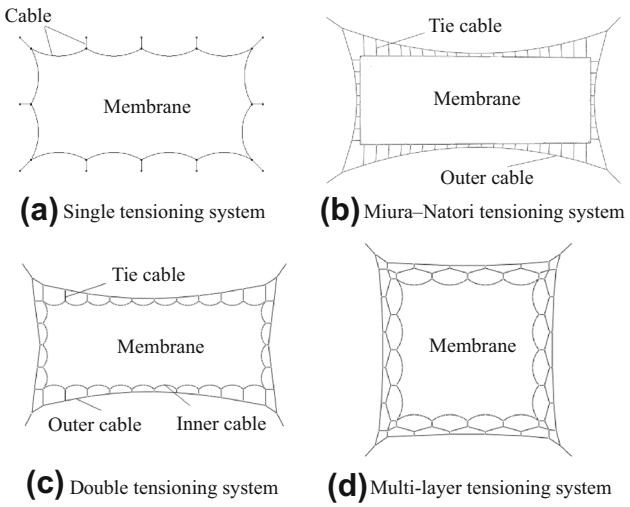

Figure 9 Different kinds of tensioning systems

5 Advances in Design and Analysis of Large Planar Membrane Antennas

5.1 Design and Analysis of Tensioning System

The tensioning system, which refers to the cables between the membrane and frame of a planar membrane antenna, provides flexible connections between these two parts and applies uniform stress to the membrane. If the tensioning system is designed improperly, the membrane will tend to wrinkle, which will impact antenna performance. In order to reduce membrane wrinkles, different tensioning systems have emerged, including the single tensioning system, Miura–Natori tensioning system, double tensioning system, and multi-layer tensioning system, as shown in Figure 9.

In 2000, Lin (of ILC Dover) et al. [43] designed the single tensioning system, as shown in Figure 8(a). The membrane edges are cut into curved pockets, in which cables can move freely. Two ends of the cable are tightened to the rectangular frame (the frame is not shown in the figure). One pocket corresponds to two tensioning points, and n pockets correspond to n tensioning points. Membranes with more pockets could get more uniform stress but the number of connection points between the membrane and frame increases simultaneously. Lin et al. [43], pointed out circular pockets could make a membrane in an isotropic tensile stress state. In 2001, however, Fang (of JPL) et al. [64], revealed that parabolic pockets could reduce membrane wrinkles. For membranes with multiple pockets, Fang et al. [64], analyzed the relationships between the cable tension force, number of pockets, and length of pockets. However, the effects of the pocket number and pocket length on the membrane effective area were not analyzed. In 2010, taking a rectangular membrane as an example, Xiao et al. [65], from Shanghai Jiao Tong University, compared parabolic and circular pockets with different rise-to-span ratios (the ratio of pocket depth to length). The results show that a membrane with parabolic pockets gets more uniform stress distribution. Only a few rise-to-span ratios were calculated in this paper, so the conclusion universality needs to be further verified.

The Miura–Natori tensioning system [66] was proposed by Koryo Miura and Michihiro Natori of the Institute of Space and Aeronautical Science (ISAS) in 1985, as shown in Figure 8(b). The straight rectangular membrane edges without pockets are connected directly with tie cables, which are connected with outer cables. Both ends of the outer cables are tightened to the rectangular frame. This tensioning system could reduce the number of connection

points between the frame and membrane, thus simplifying the frame design. However, the tie cable tension force will produce wrinkles at the membrane edges and the wrinkles will propagate to the middle of the membrane. Furthermore, so many tie cables will lead to cable winding, which will increase the risk of antenna deployment failure.

In 2003, Sakamoto et al. [67], from the University of Colorado, proposed the double tensioning system, as shown in Figure 8(c). It is equivalent to a combination of the single and Miura–Natori tensioning systems. Tie cables are connected with both the inner cables in the pockets and the outer cables tightened to the frame. After comparing the single and double tensioning systems, Sakamoto et al. [68], pointed out that when applying the same stress on the membrane, the cable mass and tension force required for the double tensioning system are smaller, and the membrane is more resistant to wrinkling, but the risk of antenna deployment failure still exists because of cable winding. In this paper, the relationships between pocket parameters and membrane anti-wrinkle ability were not analyzed. In 2008, Guan et al. [49], from Zhejiang University, optimized the number of pockets, aiming at minimizing the force loaded to the frame, and revealed that odd numbers are better than even. However, the length of the pockets and tie cables were not optimized in this paper.

In 2005, Sakamoto et al. [69], put forward the multi-layer tensioning system, which is a combination of the double tensioning system and a layer of tie cables, as shown in Figure 8(d). The two layers of tie cables are connected by some cables. Adding a layer of tie cables reduces the impact of frame vibrations on the membrane, but the cable mass and risk of deployment failure caused by cable windings will increase. Sakamoto et al. [69], performed response analysis of membrane structures to external low frequency disturbances. The results show that the multi-layer tensioning system enhanced the passive vibration isolation effect in the boundary layers. However, the optimal balance between the vibration isolation effect and cable mass was not considered in this paper.

In general, in order to apply uniform stress to the membrane, the single, double, and multi-layer tensioning systems can meet the requirements. However, connection points between the frame and membrane should be as few as possible, so the single tensioning system is not suitable for large planar membrane antennas. Double and multi-layer tensioning systems are the development tendency, and future studies are still needed for multi-objective optimizations of these two tensioning systems to reduce mass and to improve their anti-wrinkle and anti-vibration abilities.

5.2 Structural Dynamics

Planar membrane antenna performance is directly affected by the surface flatness. As a typical flexible membrane structure, its dynamic characteristics have great influence on the surface flatness. Therefore, it is necessary to perform dynamic analysis on planar membrane antenna structures. In 2007, Shen (of CSA) et al. [70], conducted modal analysis on a membrane with circular pockets with ABAQUS and found that the fundamental frequency of the membrane was directly proportional to the square root of membrane stress. In 2010, Xiao et al. [65], analyzed the fundamental frequency of rectangular membranes with different rise-to-span ratios of pockets with ABAQUS and pointed out that when the ratio decreased, the fundamental frequency of the membrane decreased slightly. In 2015, Liu et al. [71], from Xidian University, studied the influence of pocket geometry parameters on the membrane fundamental frequency and revealed that when the center angle of the pockets increased, the fundamental frequency increased. The above modal analyses only focus on the membrane instead of the whole antenna structure, which consists of the membrane, frames, and tensioning systems. In 2006, Fang et al. [72] performed numerical simulations on a model of the whole antenna structure by the distributed transfer function method, but the membrane structure geometric nonlinearity was not taken into account. In 2012, Hu et al. [73], from Shanghai Jiao Tong University, carried out modal analysis of the whole antenna structure with ABAQUS and found that membrane stress had a greater influence on the fundamental frequency than area density, but the relationships between the fundamental frequency and frame structure parameters were not analyzed.

In short, most of the current dynamic analysis of planar membrane antenna structures just focuses on antennas after deployment and on some local parts, and the membrane structure flexibility is ignored. Therefore, it is necessary to engage further study on dynamics of antennas during deployment and the rigid-flexible coupling system of the entire spacecraft.

6 Conclusions and Outlook

6.1 Conclusions

Based on the analyses mentioned above, the following conclusions can be drawn.

(1) Inflatable antennas will gradually be replaced by inflatable-rigidizable antennas because of gas leakage, short service life, etc.

(2) If the cable winding probability can be reduced and high voltage hazard can be eliminated, surface accuracy of electrostatic forming membrane antennas will be further improved based on existing Astromesh antennas. Therefore, the electrostatic forming membrane antenna will be a good candidate for a large antenna with high precision.
(3) Among the parabolic membrane antennas mentioned above, the SMP-inflatable membrane antennas have strong surface stability and high deployment reliability. If enough power can be supplied, SMP-inflatable membrane antennas will be another development trend for large-scale and high-precision antennas.
(4) Polyimide film will be a good candidate for reflector membrane materials because of its good mechanical properties, high thermal stability, and strong anti-radiation ability.
(5) Frame shapes of planar membrane reflect array antennas tend to be rectangular.
(6) Both CFRP and inflatable-rigidizable booms have promising futures in membrane SAR antenna applications.
(7) The double and multi-layer tensioning systems have the advantages of reducing the number of connection points between the frame and membrane and improving the anti-wrinkle and anti-vibration ability of membrane structures. Therefore, they will be widely used in future large planar membrane antenna applications.

6.2 Outlook

In order to realize the space applications of large membrane antennas, the following technical problems should be solved.

6.2.1 *Design and Analysis of Membrane Structures*

(1) In order to determine the shape of membrane to be cut, an inverse solution to the configuration of a membrane structure in the unstressed state should be obtained based on its desired configuration under the stressed state.
(2) Multi-parameter and multi-objective optimizations of the high precision membrane antenna structures should be performed considering the membrane material creep property and structural nonlinearity.
(3) Membrane wrinkle numerical simulation [74–76] aimed at large membrane antenna structures should be studied so that the specific locations and intensity of membrane wrinkles caused by external perturbations can be obtained, which is necessary for large membrane antenna structural design.
(4) Dynamics of rigid-flexible coupling systems, such as spacecraft structures with large membrane antenna structures, need to be further studied, along with the dynamics of antennas in the deployment process.
(5) Further research about the effects of mechanical-thermal-electrical coupling factors on membrane antenna surface accuracy should be emphasized.

6.2.2 *Materials and Processes*

(1) Wider size polyimide film manufacturing technologies should be developed to prevent membrane wrinkles, which generally exist in the connecting areas between small pieces.
(2) Polyimide film with a smaller thermal expansion coefficient and quality loss in space should be developed to improve membrane antenna dimensional stability and endurance in orbit.
(3) Technologies for metal coating on large polyimide film surfaces need to be further investigated to reduce the effect of non-uniformity on surface accuracy and reflectivity of the membrane reflector.
(4) It is necessary to further improve the performance stability and service life in orbit of current composite materials used in support structures and to develop new composite materials with higher stiffness and lighter mass for larger scale support structures.

6.2.3 *Packing Methods for Membrane Antennas*

Packing methods for membrane antennas should be studied, so that antenna storage volume and packing complexity can be reduced with no electronic device damage occurring.

6.2.4 *Surface Accuracy Stability in Orbit*

The surface accuracy maintaining system consists of a surface measuring system [77], a control system, and actuators placed on the reflector surface [78, 79]. It is necessary to look for a way to increase the measuring system accuracy, improve the control system algorithms that consider membrane material creep properties and structural nonlinearity, and optimize the actuator numbers and configurations.

6.2.5 *Test and Verification Technology*

It is important to develop a method for minimizing the effect of ground microgravity simulation systems on the

experimental measurement results for lightweight and flexible membrane antenna structures in the future.

References

1. H L Huang, Z Q Deng, B Li. Mobile assemblies of large deployable mechanisms. *Journal of Space Engineering*, 2012, 5(1): 1–14.
2. Z R Chu, Z Q Deng, X Z Qi, et al. Modeling and analysis of a large deployable antenna structure. *Acta Astronautica*, 2014, 95(1): 51–60.
3. S N Lu, D Zlatanov, X L Ding, et al. A new family of deployable mechanisms based on the Hoekens linkage. *Mechanism and Machine Theory*, 2014, 73: 130–153.
4. S N Lu, D Zlatano, X L Ding, et al. A network of type III Bricard linkages. *ASME 2015 International Design Engineering Technical Conferences and Computers and Information in Engineering Conference*, Boston, Massachusetts, August 2–5, 2015.
5. X L Ding, X Li. Design of a type of deployable/retractable mechanism using friction self-locking joint units. *Mechanism and Machine Theory*, 2015, 92: 273–288.
6. Y S Zou, G F Ding, W Zhang, et al. Collaborative simulation method with spatiotemporal synchronization process control. *Chinese Journal of Mechanical Engineering*, 2016, 29(6): 1074–1082.
7. G Carbone. Experimental characterization of a binary actuated parallel manipulator. *Chinese Journal of Mechanical Engineering*, 2016, 29(3): 1–9.
8. L J Zhang, F Guo, Y Q Li, et al. Global dynamic modeling of electro-hydraulic 3-UPS/S parallel stabilized platform by bond graph. *Chinese Journal of Mechanical Engineering*, 2016, 29(6): 1176–1185.
9. K Xu, L Li, S P Bai, et al. Design and analysis of a metamorphic mechanism cell for multistage orderly deployable/retractable mechanism. *Mechanism and Machine Theory*, 2017, 111: 85–98.
10. S N Lu, D Zlatano, X L Ding. Approximation of cylindrical surfaces with deployable bennett networks. *Journal of Mechanisms and Robotics*, 2017, 9(2): 021001-021001-6.
11. F C Qin, Y T Li, H P Qi, et al. Advances in compact manufacturing for shape and performance controllability of large-scale components-a review. *Chinese Journal of Mechanical Engineering*, 2017, 30(1): 7–21.
12. C G Cassapakis, A W Love, A L Palisoc. Inflatable space antennas-a brief overview. *IEEE Proceedings of the 1998 IEEE Aerospace Conference*, Aspen, Colorado, March 21–28, 1998: 453–459.
13. Y Rahmat-Samii, A Densmore. A history of reflector antenna development: Past, present and future. *IEEE International Microwave and Optoelectronics Conference*, 2009: 17–23.
14. J G Liu, S F Sun. A brief survey on inflatable deployment space structures' research and development. *International Conference on Reconfigurable Mechanism and Robots*, Tianjin, China, July 9–11, 2012: 773–782.
15. J C Pearson, R R Romanofsky. Thin film antenna development and optimization. *47th AIAA/ASME/ASCE/AHS/ASC Structures, Structural Dynamics, and Materials Conference*, Newport, Rhode Island, May 1–4, 2006.
16. E Im, M Thomson, H Fang. Prospects of large deployable reflector antennas for a new generation of geostationary Doppler weather radar satellites. *AIAA Space 2007 Conference and Exposition*, Long Beach, California, September 18–20, 2007.
17. R E Freeland, G D Biilyeu, G R Veal. Development of flight hardware for a large, inflatable-deployable antenna experiment. *Acta Astronautica*, 1996, 38(4–8): 251–260.
18. R E Freeland, G D Bilyeu, G R Veal, et al. Large inflatable deployable antenna flight experiment results. *Acta Astronautica*, 1997, 41(4): 267–277.
19. R E Freeland, G R Veal. Significance of the inflatable antenna experiment technology. *39th AIAA/ASME/ASCE/AHS/ASC Structures, Structural Dynamics, and Materials Conference and Exhibit*, Long Beach, California, Apr 20–23, 1998.
20. G Greschik, A Palisoc, C Cassapakis, et al. Sensitivity study of precision pressurized membrane reflector deformations. *AIAA Journal*, 2001, 39(2): 308–314.
21. S Naboulsi. Investigation of geometric imperfection in inflatable aerospace structures. *Journal of Aerospace Engineering*, 2004, 17(3): 98–105.
22. Y Xu, F L Guan, Y Guan. Precision analysis and shape adjustment of inflatable antenna. *Chinese Journal of Space Science*, 2006, 26(4): 292–297. (in Chinese)
23. M J Coleman, F Baginski, R R Romanofsky. Effect of boundary support and reflector dimensions on inflatable parabolic antenna performance. *Journal of Spacecraft and Rockets*, 2012, 49(5): 905–914.
24. F S Liu, D P Jin. Analytical Investigation of dynamics of inflatable parabolic membrane reflector. *Journal of Spacecraft and Rockets*, 2015, 52(1): 285–294.
25. C Cassapakis, M Thomas. Inflatable structures technology development overview. *AIAA Space Programs and Technologies Conference*, Huntsville, AL, September 26–28, 1995.
26. X F Ma, Y P Song, J F Wei, et al. Review on the structure of inflatable space antennas. *Space Electronic Technology*, 2006, (3): 10–15. (in Chinese)
27. C Y Lai, S Pellegrino. Deployable membrane reflectors with offset configuration. *40th AIAA/ASME/ASCE/AHS/ASC Structures, Structural Dynamics*, and Materials Conference, Saint Louis, Missouri, Apr 12–15, 1999.
28. K A Seffen, Z You, S Pellegrino. Folding and deployment of curved tape springs. *International Journal of Mechanical Sciences*, 2000, 42(10): 2055–2073.
29. S Pellegrino. Deployable membrane reflectors. *2nd World Engineering Congress*, Sarawak, Malaysia, 2002: 1–9.
30. J K H Lin, H Fang, E Im, et al. Concept study of a 35-m spherical reflector system for NEXRAD in space application. *47th AIAA/ASME/ASCE/AHS/ASC Structures, Structural Dynamics, and Materials Conference*, Newport, Rhode Island, May 1–4, 2006.
31. Y J Liu, H Y Du, L W Liu, et al. Shape memory polymers and their composites in aerospace applications: a review. *Smart Materials and Structures*, 2014, 23(2): 23001–230222.
32. J L Gaspar, Mann T, T Sreekantamurthy, et al. Structural test and analysis of a hybrid inflatable antenna. *48th AIAA/ASME/ASCE/AHS/ASC Structures, Structural Dynamics, and Materials Conference*, Honolulu, Hawaii, Apr 23–26, 2007.
33. O S Alvarez-Salazar, D Adams, M Milman, et al. Pointing architecture of SMAP's large spinning antenna. *AIAA Guidance, Navigation and Control (GNC) Conference*. Boston, Massachusetts, August 19–22, 2013.
34. S P Chodimella, J D Moore, J Otto, et al. Design evaluation of a large aperture deployable antenna. *47th AIAA/ASME/ASCE/AHS/*

ASC Structures, Structural Dynamics, and Materials Conference, Newport, Rhode Island, May 1–4, 2006.
35. Y Q Zhang, F Gao, S X Zhang, et al. Electrode grouping optimization of electrostatic forming membrane reflector antennas. *Aerospace Science and Technology*, 2015, 41: 158–166.
36. C Liu, G G Yang, Y Q Zhang. Optimization design combined with coupled structural-electrostatic analysis for the electrostatically controlled deployable membrane reflector. *Acta Astronautica*, 2015, 106: 90–100.
37. J C Pearson, J D Moore, H Fang. Large and high precision inflatable membrane reflector. *51st AIAA/ASME/ASCE/AHS/ASC Structures, Structural Dynamics, and Materials Conference*, Orlando, Florida, Apr 12–15, 2010.
38. J G Liu, H J Ni, H Gao, et al. Research and application of ultrathin polyimide films. *Spacecraft Environment Engineering*, 2014, 31(5): 470–475. (in Chinese)
39. G Rait, D Beasley. Large area membrane apertures for space applications, fabrication and mechanical testing. *4th AIAA Spacecraft Structures Conference*, Grapevine, Texas, January 9–13, 2017.
40. J Huang. The development of inflatable array antennas. *Antennas and Propagation Magazine*, 2001, 43(4): 44–50.
41. J Hang, A Feria. A One-meter X-band inflatable reflectarray Antenna. *Microwave and Optical Technology Letters*, 1999, 20(2): 97–99.
42. D P Cadogan, J K Lin, M S Grahne. The development of inflatable space radar reflectarrays. *Proceedings of the 40th AIAA/ ASME/ ASCE/AHS/ASC Structures, Structural Dynamics, and Materials Conference and Exhibit*, Saint Louis, Missouri, Apr 12–15, 1999.
43. J K H Lin, D P Cadogan, V A Feria, et al. An inflatable Microstrip Reflectarray concept for Ka-band applications. *41st AIAA/ASME/ASCE/AHS/ASC Structures, Structural Dynamics, and Materials Conference and Exhibit*, Atlanta, GA, Apr 3–6, 2000.
44. H Fang, M Lou, J Huang, et al. Development of a three-meter Ka-band reflectarray antenna. *43rd AIAA/ASME/ASCE/AHS /ASC Structures, Structural Dynamics, and Materials Conference*, Denver, Colorado, Apr 22–25, 2002.
45. J Huang, H Fang, R Lovick, et al. The development of large flat inflatable antenna for deep-space communications. *Space 2004 Conference and Exposition*, San Diego, California, Sep 28–30, 2004.
46. H Fang, M Lou, J Huang, et al. Development of a 7-meter inflatable reflectarray antenna. *45th AIAA/ASME/ASCE/AHS/ASC Structures, Structural Dynamics, and Materials Conference*, Palm Springs, California, Apr 19–22, 2004.
47. H Fang, J Huang, Q Ubaldo. Design and technologies development for an eight-meter inflatable reflectarray antenna. 47*th AIAA/ASME/ASCE/AHS/ASC Structures, Structural Dynamics, and Materials Conference*, Newport, Rhode Island, May 1–4, 2006.
48. H Fang, K Knarr, U Quijano, et al. In-space deployable reflectarray antenna: Current and future. *49th AIAA/ASME/ASCE/AHS/ASC Structures, Structural Dynamics, and Materials Conference*, Schaumburg, IL, Apr 7–10, 2008.
49. F L Guan, Y W Wang, C H Yang. Design and fabrication of new type reflect array antenna. *Journal of Engineering Design*, 2008, 15(6): 466–471. (in Chinese)
50. X Q Li, X F Zheng, C Yang. Design on double frequency and wide band microstrip reflectarray antenna. *Journal of Microwaves*, 2012, 28(1): 8–11. (in Chinese)
51. M C Lou, V Feria. Development of an inflatable space synthetic aperture radar. *39th AIAA/ASME/ASCE/AHS/ASC Structures, Structural Dynamics, and Materials Conference and Exhibit*, Long Beach, California, Apr 20–23, 1998.
52. Y Wang, Z Q Deng, R Q Liu, et al. Topology structure synthesis and analysis of spatial pyramid deployable truss structures for satellite SAR antenna. *Chinese Journal of Mechanical Engineering*, 2014, 27(4): 83–692.
53. C S Wang, R B Han, W Wang. Development of spaceborne deployable active phased array antennas. *Journal of Mechanical Engineering*, 2016, 52(5): 107–123. (in Chinese)
54. B C Lopez, M C Lou, J Huang, et al. Development of an inflatable SAR engineering model. *42nd AIAA/ASME/ASCE/ AHS/ASC Structures, Structural Dynamics, and Materials Conference and Exhibit*, Seattle, Washington, Apr 16–19, 2001.
55. M Lou, H Fang, L M Hsia. Self-rigidizable space inflatable boom. *Journal of Spacecraft and Rockets*, 2002, 39(5): 682–690.
56. H Fang, M Lou, J Hah. Deployment study of a self-rigidizable inflatable boom. *Journal of Spacecraft and Rockets*, 2006, 43(1): 25–30.
57. A Moussessian, L Del Castillo, V Bach, et al. Large aperture, scanning, L-band SAR. *NASA Earth Science Technology Conference*, Pasadena, California, June 21, 2011.
58. J C Heald, M J Potvin, X X Jiang. Experimental investigations to support a multi-layer deployable membrane structure for space antennae. *46th AIAA/ASME/ASCE/AHS/ASC Structures, Structural Dynamics, and Materials Conference*, Austin, Texas, Apr 18–21, 2005.
59. Y Shen, S Montminy, W Zheng, et al. Large SAR membrane antenna deployable structure design and dynamic simulation. *48th AIAA/ASME/ASCE/AHS/ASC Structures, Structural Dynamics, and Materials Conference*, Honolulu, Hawaii, Apr 23–26, 2007.
60. M J Potvin, S Montminy, S Brunel, et al. Testing of a deployable SAR membrane antenna mechanical prototype. *49th AIAA / ASME/ASCE/AHS/ASC Structures, Structural Dynamics, and Materials Conference*, Schaumburg, Illinois, Apr 7–10, 2008.
61. M Straubel, J Block, M Sinapius, et al. Deployable composite booms for various gossamer space structures. *52nd AIAA/ASME/ ASCE /AHS/ASC Structures, Structural Dynamics, and Materials Conference*, Denver, Colorado, Apr 4–7, 2011.
62. M Straubel, P Seefeldt, P Spietz, et al. The design and test of the Gossamer-1 boom deployment mechanisms engineering model. *2nd AIAA Spacecraft Structures Conference*, Kissimmee, Florida, January 5–9, 2015.
63. M Straubel, C Huhne, C Arlt, et al. Design and sizing of a 40m^2 deployable membrane SAR space antenna. *12th European Conference on Spacecraft Structures, Materials and Environmental Testing*, Noordwijk, The Netherlands, March 20–23, 2012.
64. H Fang, M Lou, L M Hsia, et al. Catenary systems for membrane structures. *42nd AIAA/ASME/ASCE/AHS/ASC Structures, Structural Dynamics, and Materials Conference and Exhibit*, Seattle, Washington, Apr 16–19, 2001.
65. W W Xiao, W J Chen, G Y Fu. Pre-stress introduction effects and influence factors investigation for the space planar film reflectarray. *Journal of Astronautics*, 2010, 31(3): 845–849. (in Chinese)
66. K Miura, M Natori. 2-D array experiment on board a space flyer unit. *Space Solar Power Review*, 1985, 5(4): 345–356.
67. H Sakamoto, Y Miyazaki, K C Park. Evaluation of cable suspended membrane structures for wrinkle-free design. *44th AIAA/ ASME/ASCE/AHS/ASC Structures, Structural Dynamics, and Materials Conference*, Norfolk, Virginia, Apr 7–10, 2003.
68. H Sakamoto, K C Park, Y Miyazaki. Dynamic wrinkle reduction strategies for cable-suspended membrane structures. *Journal of Spacecraft and Rockets*, 2005, 42(5): 850–858.
69. H Sakamoto, K C Park. Advanced cable boundary layer design in membrane structures for dynamic wrinkle reduction. *46th AIAA/ ASME/ASCE/AHS/ASC Structures, Structural Dynamics, and Materials Conference*, Austin, Texas, Apr 18–21, 2005.

70. Y Shen, W P Zheng, X Y Wang. Dynamic and vibration analysis of a SAR membrane antenna. *ASME International Mechanical Engineering Congress and Exposition*, 2007: 17–24.
71. C Liu, Y H Li, H Bao, et al. Natural frequencies of pre-tensioned membrane structure with different boundary geometrical parameters. *Journal of Vibration and Shock*, 2015(20): 198–202. (in Chinese)
72. H F Fang, B G Yang, H L Ding, et al. Dynamic analysis of large in-space deployable membrane antennas. *The 13th International Congress on Sound and Vibration*, Vienna, Austria, July, 2006.
73. Y Hu. *Analysis of pre-stress and structural characteristic of space film reflect-array*. Shanghai: Shanghai Jiao Tong University, 2012. (in Chinese)
74. X W Du, C G Wang, Z M Wan. Advances of the study on wrinkles of space membrane structures. *Advances in Mechanics*, 2006, 36(2): 187–199. (in Chinese)
75. K Senda, M Petrovic, K Nakanishi. Wrinkle generation without bifurcation in a shear-enforced rectangular membrane with free boundaries. *Journal of Spacecraft and Rockets*, 2015, 52(4): 1057–1073.
76. X F Wang, J Ma, S S Law, et al. Numerical analysis of wrinkle-influencing factors of thin membranes. *International Journal of Solids & Structures*, 2016, 97–98(2006): 458–474.
77. Y Shimoda, K Watanabe, N Sakamoto, et al. Development of Stereo Camera System for Accurate Observation of Deployable Membranes onboard CubeSat. *55th AIAA Aerospace Sciences Meeting*, Grapevine, Texas, January 9–13, 2017.
78. J R Hill, K W Wang, H Fang, et al. Actuator grouping optimization on flexible space reflectors. *SPIE International Society for Optics and Photonics*, San Diego, California, March 7–10, 2011.
79. X B Chen, F Gao, C K Qi, et al. Gait planning for a quadruped robot with one faulty actuator. *Chinese Journal of Mechanical Engineering*, 2015, 28(1): 11–19.

Zhi-Quan Liu, born in 1963, is currently a professor and a PhD candidate supervisor at *China Academy of Space Technology, China*. He received his PhD degree from *Harbin Institute of Technology, China*, in 1996, completed post-doctoral study at *Northwestern Polytechnical University, China*, in 1998. His research interests include spacecraft structure and mechanism design, spacecraft reliability technology. Tel: +86-10-68747342; E-mail: liuzhiquanymj@sina.com.

Hui Qiu, born in 1992, is currently a master student at *China Academy of Space Technology, China*. She received her bachelor degree from *School of Astronautics, Beihang University, China*, in 2010. Her research interests include spacecraft structure and mechanism design. Tel: +86-10-68745721; E-mail:qh_sofa@126.com.

Xiao Li, born in 1982, is currently an engineer at *China Academy of Space Technology, China*. He received his master degree from *Beihang University, China*, in 2005. His research interests include mechanical design and analysis. Tel: +86-10-68111279; E-mail: lixiao_cast@hotmail.com.

Shu-Li Yang, born in 1982, is currently an engineer at *China Academy of Space Technology, China*. She received her PhD degree from *China Academy of Space Technology, China*, in 2014. Her research interests include spacecraft structure and mechanism design. Tel: +86-10-68745717; E-mail: cast5041@gmail.com.